Direct fabrication of single-walled carbon nanotube macro-films on flexible substrates†

Hongwei Zhu and Bingqing Wei*

Received (in Berkeley, CA, USA) 16th February 2007, Accepted 5th April 2007
First published as an Advance Article on the web 20th April 2007
DOI: 10.1039/b702523h

We employed a floating chemical vapor deposition technique and applied a liquid (solution)-free precursor system for the fabrication of single-walled carbon nanotube macro-films on various flexible substrates from metallic foils to polymer films.

The ultimate goal of current research on carbon nanotubes is to make breakthroughs that advance nanotechnological applications of bulk nanotube materials. There has been growing interest in film-like nanotube macrostructures because of their unique and usually enhanced properties and tremendous potential as components for use in nano-electronic and nano-mechanical device applications or as structural elements in various devices.[1,2] For example, carbon nanotube macro-films are expected to have excellent properties implying promising applications. Self-assembled nanotube networks in these films will facilitate the device fabrication process and would provide the opportunities in creating a revolutionary new class of nano devices, such as mechanical actuators,[3] filters[4] and nanotube-filled composites.[5] Especially, in energy storage systems, carbonaceous materials electrodes have been commonly used in supercapacitors, fuel cells, batteries and other electrochemical applications.[6] Advantages of considering nanotube films for these applications are their uniform dimensions, large specific surface area and smooth surface topology. If a synthetic method can directly produce a large yield of nanotube macro-films, these films will not only be used to verify fundamental properties of the nano-featured bulk materials but also have tremendous potential for practical applications in the above-mentioned devices.

A primary objective of the present work is to provide a novel process of direct deposition of nanotube macro-films on flexible substrates. Various methods were already demonstrated to prepare continuous macroscopic structures of carbon nanotubes during direct synthesis[1] and post-treatment process.[2] However, the creation of macro-films of single-walled carbon nanotubes (SWNTs) with controllable dimension by self-assembly/direct deposition still remains a challenge. Super-long SWNT strands have been synthesized by an optimized synthetic method in our group, which also promoted and promised a mass production of SWNT macro-films in an efficient and cost-effective way. Here, we report that we have succeeded in preparing macro-films of SWNTs directly on various flexible substrates (copper, stainless steel, aluminium, nickel mesh foils and polymer films, see ESI,† Fig. S2) by applying a liquid (solution)-free precursor system, in which ferrocene and sulfur powders were mixed uniformly.

SWNT macro-films were grown by a simple floating chemical vapor deposition (CVD) method using ferrocene as carbon feedstock/catalyst and sulfur as an additive to promote SWNT growth to a high percentage. There is no additional carbon source (*e.g.* xylene, hexane and methane) required for the synthesis. The schematic of the SWNT synthesis setup is shown in Fig. S1, ESI.† It is an adaptation of the CVD technique used previously for the production of SWNTs and essentially a one-step process. By varying the growth conditions (such as the growth temperature, flow rate of buffer gas, composition of ferrocene/sulfur), the nanotubes can be controlled to be single-walled. In detail, a solid volatile mixture of ferrocene and sulfur (atomic ratio Fe : S = 10 : 1) was introduced into one end of a ceramic tube (total 150 cm in length, 7 cm inner diameter). An argon flow with rate of 200 mL min^{-1} was then passed through the furnace tube and the furnace was heated to 1100–1150 °C. The ceramic tube was moved so as to locate the mixture within the furnace. After 10–30 min reaction duration under a gas flow of argon (1500 mL min^{-1}) and hydrogen (150 mL min^{-1}) mixture, the furnace was allowed to cool to room temperature. The SWNT samples were characterized by scanning electron microscopy (SEM, Hitachi S3600N), transmission electron microscopy (TEM, JEOL JEM 2010, at an accelerating voltage of 200 kV) and Raman Microscope (Labram 300, Horiba Jobin Yvno Inc.) with the excitation of 633 nm laser (17 mW) to determine surface morphology, thickness, purity and tube diameter distribution, *etc.*

The highly stable conditions in the reactor allow an undisturbed SWNT growth/deposition in a continuous manner with an accurate control of the film thickness even on complex substrates with deformities. A reaction tube with large inner diameter was used here to generate a reverse-flowing gas flow of argon and hydrogen. Therefore, besides on the inner wall of the rear half of the reaction tube, the nanotube macro-films were also deposited on the inner wall of the front half, as shown schematically in Fig. 1(a), suggesting the existence of a reverse gas flow due to the pressure difference between the tube center and the cold ends. Thus the whole reaction tube can be fully utilized to collect the nanotube products, leading to macroscopic films with large area uniformity and conformity. Direct deposition of nanotube macro-films on various substrates was realized by placing these substrates at the 60–800 °C zone (total 100 cm wide) before growth and clinging them closely to the inner wall of the reaction tube. The temperature range for film deposition may possibly be extended to still lower temperatures by increasing the length of the reaction tube. The wide deposition zone allows large-area film coverage

Department of Mechanical Engineering, University of Delaware, Newark, DE 19716, USA. E-mail: weib@udel.edu; Fax: +1 302 8313619; Tel: +1 302 8316438

† Electronic supplementary information (ESI) available: Materials and methods, additional figures and movies. See DOI: 10.1039/b702523h

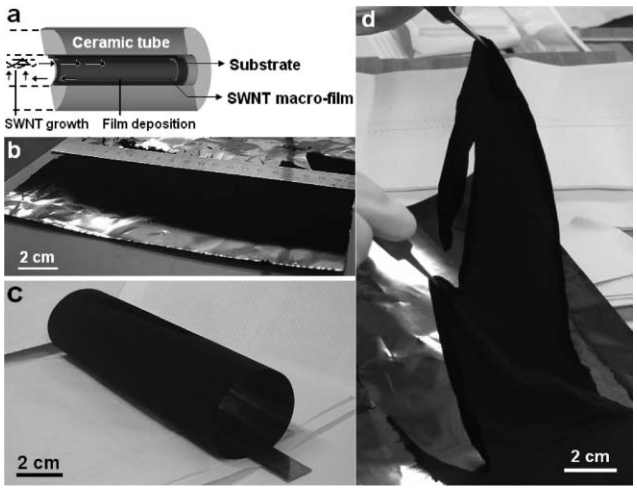

Fig. 1 Photographs of SWNT macro-films. (a) Schematic of substrate assembly and SWNT macro-film deposition on the inner wall of the front end of the reactor. (b) As-received SWNT macro-film and (c) a rolled up SWNT macro-film deposited on a stainless steel foil. (d) A lift-up SWNT macro-film peeled off from the substrate.

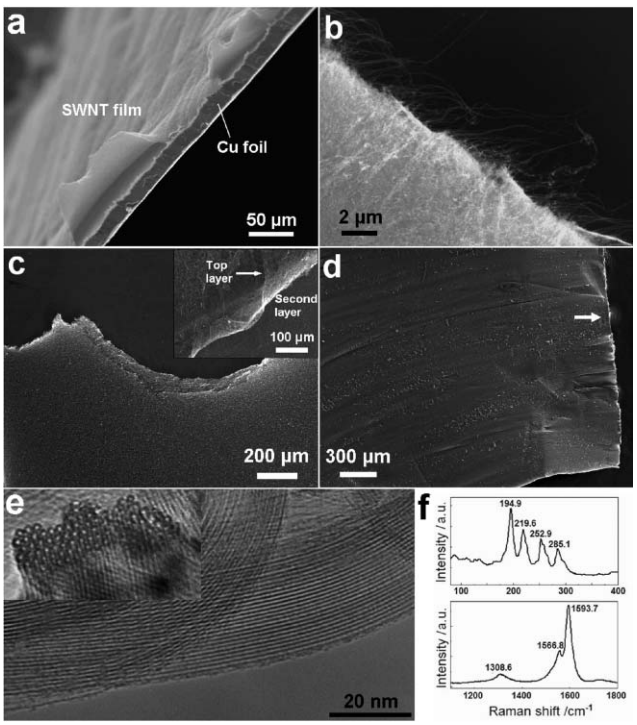

Fig. 2 Electron microscopy and Raman characterizations of SWNT macro-films. (a) A SWNT film deposited on a copper foil. (b) Protruded SWNT bundles. (c) Layered structure. Inset: a peeled-off SWNT layer. (d) SWNT film cut with scissors. (e) Lateral view of a SWNT bundle. Inset: a cross-section view of a SWNT bundle. (f) Raman spectra of SWNT films.

without damaging substrate materials, especially for those that cannot stand a high temperature (for instance, polymer and aluminium). It should be mentioned here the SWNT growth and film deposition took place separately. SWNTs were first grown at the hot zone of the reactor and then carried by the buffer gas to the cool ends and deposited on the substrates. The deposition showed no difference and SWNT films have same features in terms of nanotube structures and morphologies, and therefore, hold the same properties on all the substrates. The film area can be up to 200 cm^2 which represents the highest values ever reported from a direct synthesis technique.

The as-deposited SWNT film exhibits a perfect structural uniformity and flexibility (as shown in Fig. 1(b)–(d) and ESI,† Movie S1). Most importantly, the nanotube macro-films could be peeled off from substrates and transferred to other substrates without any damage. SEM images provide detailed information about the thickness and surface morphology of the SWNT macro-films. A 5 μm thick SWNT film deposited on a copper foil is presented in Fig. 2(a). A semi-transparent film on a nickel mesh in a high magnification SEM image showing SWNT bundles is also provided in Fig. S2 of ESI†). Entangled nanotube bundles can be clearly imaged at the edge of the SWNT films [Fig. 2(b)]. The thickness of the films can be controlled in a straightforward manner by controlling the deposition time. An interesting multi-layered structure was identified by partially removing the first layer of the SWNT film, as seen in Fig. 2(c). The inset of Fig. 2(c) shows that the top layer of the film was peeled off with tweezers and the underneath layer could be exposed. The formation of multi-layered structure is probably due to the fluctuation of gas flow during growth which is associated with different deposition sub-cycles. Simple cutting and punching (see ESI,† Fig. S3) could be used to cut and trim the film uniformly into any desired shape for various applications. Fig. 2(d) shows the smooth side (indicated by a white arrow) of a SWNT film after the cutting process. TEM characterizations suggest that the SWNT macro-films are composed of entangled SWNT bundles and a certain amount of impurities, including amorphous carbon and catalytic iron nanoparticles (~20 wt% based on the EDX result). There are no multi-walled carbon nanotubes found in the samples. The size of the catalytic nanoparticles ranged from 1 to 10 nm based on the TEM measurements. A typical TEM image is shown in Fig. S4 of ESI.† As mentioned before, the growth and the deposition in our approach are two separate processes. During the growth, when individual SWNTs incorporate together to form a bundle, the catalytic nanoparticles would be relatively large particles. However, there is no direct correlation between an individual nanotube diameter and the size of the catalytic nanoparticles. Also, the deposition gives no difference on all substrates and there appeared to be no relation between the catalyst size and the substrates. Two typical high-resolution TEM images of SWNT bundles are shown in Fig. 2(e), demonstrating the well-known two-dimensional triangular crystal structure. We obtained an estimation of the diameter distribution of SWNTs using Raman with a 633 nm excitation. Fig. 2(f) shows the Raman spectra of SWNT macro-films. The most important feature in the Raman spectra of SWNTs is the radial breathing mode (RBM), which is usually located between 75 and 300 cm^{-1}.[7] The frequency of the RBM (ω) is directly linked to the reciprocal of the nanotube diameter (d): ω (cm^{-1}) = 238/d (nm) $^{0.93}$. RBM analysis revealed that the nanotube diameters are widely distributed and four different diameters dominate the samples ranging from 0.8 to 1.3 nm. This estimation has been confirmed with the TEM characterizations, as shown in Fig. 2(e) and Fig. S4 of ESI.† The D band located around 1300 cm^{-1} is due to disorder-induced features or defects in the nanotubes. The G mode corresponds to the tangential

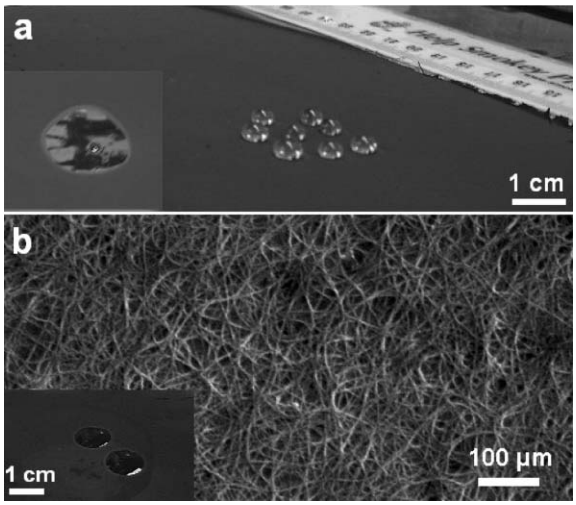

Fig. 3 Tunable surface properties of SWNT films between hydrophobic and hydrophilic. (a) As-deposited SWNT film with a hydrophobic surface, indicated by standing water droplets. Inset: an ethanol droplet wetting the SWNT film surface. (b) Purified SWNT film with a hydrophilic surface. Inset: two spreading water droplets.

displacement C–C bond stretching motions in the graphite plane which is located between 1500 and 1600 cm^{-1}. The G bands exhibit an asymmetric broadening to low frequency, which indicates the resonant scattering of the metallic components under this excitation.

The as-deposited nanotube films possess a hydrophobic surface, as shown in Fig. 3(a) and ESI,† Movie S2), while exhibiting a good affinity for most organic solvents (for example, ethanol, acetone) and can be wetted forming an organic thin film on the surface [see inset of Fig. 3(a) and ESI,† Movie S3]. This phenomenon allows us to use ethanol or acetone to enhance the adhesion between the SWNT films and the substrates. It is well known that the presence of oxygen-containing functional groups determines the wetting ability of the material to associate with water. Fully reconfigurable hydrophobic–hydrophilic surfaces can be achieved by the post purification which employed a combination of oxidations (heat in air at 450 °C for 1 h or immersion in 30% H_2O_2 solution for 72 h) and rinsing with diluted acid (37% HCl).[8] This procedure significantly reduced the amount of impurities and increased the number of functional groups (*e.g.* O=C–OH) within the film. The resulting film consists solely of SWNT bundles and shows a hydrophilic surface, as shown in Fig. 3(b). The contact angle shown in Fig. 3(b) is $\sim 10^{\circ}$, indicating a strong hydrophilic surface of the treated SWNT film. The hydrophobic surface can be regained by annealing the purified film at high temperature (>500 °C) in a vacuum or under the protection of an argon flow.

In summary, we report for the first time, the direct deposition of SWNT macro-films with controllable dimensions through modification of a simple CVD method. This work provided a simple and cost-effective way to deposit large-area SWNT films on flexible substrates. First, the precursor system contains only two components: ferrocene and sulfur, no liquid or additional carbon source (*e.g.* xylene, hexane and methane) are required. In contrast to the two-stage furnace setup,[1] this is a one-step deposition. Secondly, this work realized for the first time, the direct deposition of SWNT macro-films on various flexible substrates from metallic foils to polymer films. Thirdly, the SWNT film can be prepared to up to 200 cm^2 with our facility and can be peeled off and transferred to other substrates without any damage. The presented CVD synthesis of SWNT macro-films is highly repeatable and scalable. The successful fabrication of the SWNT macro-films open a possibility to study their intrinsic properties and anisotropic behaviors at the macroscopic scale. The integrity and stability of the nanotube macro-films are the most attractive merits for developing nano-featured macro-scale devices. Our future research starting from nanotube macro-films will include large-scale production, characterizations of their mechanical, electrical, physical and chemical properties, and exploring their potential applications. It is expected that these nanotube films will show comparable or more advantages than regular nanotubes in powder form and will be ideal structures in various applications in composites, field emission, super-capacitors, lithium batteries, optoelectronics, *etc.*

Notes and references

1 (*a*) H. W. Zhu, C. L. Xu, D. H. Wu, B. Q. Wei, R. Vajtai and P. M. Ajayan, *Science*, 2002, **296**, 884; (*b*) Y. L. Li, I. A. Kinloch and A. H. Windle, *Science*, 2004, **304**, 276; (*c*) J. Q. Wei, B. Jiang, D. H. Wu and B. Q. Wei, *J. Phys. Chem. B*, 2004, **108**, 8844; (*d*) L. Song, L. Ci, L. Lu, Z. P. Zhou, X. Q. Yan, D. F. Liu, H. J. Yuan, Y. Gao, J. X. Wang, L. F. Liu, X. W. Zhao, Z. X. Zhang, X. Y. Dou, W. Y. Zhou, G. Wang, C. Y. Wang and S. S. Xie, *Adv. Mater.*, 2004, **16**, 1529.

2 (*a*) M. Zhang, S. L. Fang, A. A. Zakhidov, S. B. Lee, A. E. Aliev, C. D. Williams, K. R. Atkinson and R. H. Baughman, *Science*, 2005, **309**, 1215; (*b*) M. Endo, H. Muramatsu, T. Hayashi, Y. A. Kim, M. Terrones and M. S. Dresselhaus, *Nature*, 2005, **433**, 476; (*c*) M. Zhang, K. R. Atkinson and R. H. Baughman, *Science*, 2004, **306**, 1358; (*d*) Z. C. Wu, Z. H. Chen, X. Du, J. M. Logan, J. Sippel, M. Nikolou, K. Kamaras, J. R. Reynolds, D. B. Tanner, A. F. Hebard and A. G. Rinzler, *Science*, 2004, **305**, 1273; (*e*) L. M. Ericson, H. Fan, H. Q. Peng, V. A. Davis, W. Zhou, J. Sulpizio, Y. H. Wang, R. Booker, J. Vavro, C. Guthy, A. N. G. Parra-Vasquez, M. J. Kim, S. Ramesh, R. K. Saini, C. Kittrell, G. Lavin, H. Schmidt, W. W. Adams, W. E. Billups, M. Pasquali, W. F. Hwang, R. H. Hauge, J. E. Fischer and R. E. Smalley, *Science*, 2004, **305**, 1447; (*f*) J. Q. Wei, L. J. Ci, B. Jiang, Y. H. Li, X. F. Zhang, H. W. Zhu, C. L. Xu and D. H. Wu, *J. Mater. Chem.*, 2003, **13**, 1340.

3 A. M. Fennimore, T. D. Yuzvinsky, W. Q. Han, M. S. Fuhrer, J. Cumings and A. Zettl, *Nature*, 2003, **424**, 408.

4 M. Majumder, N. Chopra, R. Andrews and B. J. Hinds, *Nature*, 2005, **438**, 44.

5 A. B. Dalton, S. Collins, E. Munoz, J. M. Razal, V. H. Ebron, J. P. Ferraris, J. N. Coleman, B. G. Kim and R. H. Baughman, *Nature*, 2003, **423**, 703.

6 (*a*) A. S. Arico, P. Bruce, B. Scrosati, J. M. Tarascon and S. W. Van, *Nat. Mater.*, 2005, **4**, 366; (*b*) V. H. Ebron, Z. W. Yang, D. J. Seyer, M. E. Kozlov, J. Oh, H. Xie, J. Razal, L. J. Hall, J. P. Ferraris, A. G. MacDiarmid and R. H. Baughman, *Science*, 2006, **311**, 1580.

7 S. Rols, A. Righi, L. Alvarez, E. Anglaret, R. Almairac, C. Journet, P. Bernier, J. L. Sauvajol, A. M. Benito, W. K. Maser, E. Munoz, M. T. Martinez, G. F. de la Fuente, A. Girard and J. C. Ameline, *Eur. Phys. J. B*, 2000, **18**, 201.

8 J. Q. Wei, H. W. Zhu, Y. H. Li, B. Chen, Y. Jia, K. L. Wang, Z. C. Wang, W. J. Liu, J. B. Luo, M. X. Zheng, D. H. Wu, Y. Q. Zhu and B. Q. Wei, *Adv. Mater.*, 2006, **18**, 1695.

